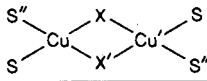


Table IV. Geometric Parameters for $\text{Cu}_2\text{X}_2\text{S}_4$ (X = Br, I)


	Br			I		
	1	3 ^a		2	4 ^b	5 ^b
Cu-X	2.451 (4)	2.456 (1)	2.463 (1)	2.574 (5)	2.575 (2)	2.594 (3)
Cu-X'	2.417 (3)	2.482 (1)	2.421 (1)	2.605 (5)	2.583 (1)	
Cu-S	2.374 (5)	2.431 (2)	2.390 (2)	2.434 (5)	2.420 (4)	2.435 (7)
Cu-S''	2.500 (4)	2.393 (2)	2.399 (2)	2.474 (5)	2.417 (3)	
Cu...Cu'	2.880 (3)	2.697 (2)		2.732 (3)	2.752 (2)	2.765 (5)
X...X'	3.925 (3)	4.013 (1)		4.313 (2)	4.363 (1)	4.391 (4)
Co...Cu	3.365 (3)	3.330 (1)	3.286 (1)	3.348 (1)	3.330 (9)	3.301 (5)
Cu-X-Cu'	72.53 (9)	66.50 (4)	66.73 (4)	63.67 (8)	64.5 (2)	64.4 (1)
S-Cu-S''	85.6 (1)	86.50 (6)	88.98 (7)	85.9 (2)	87.2 (4)	87.7 (2)

^a Reference 2. ^b Reference 3.

Table V. X-ray Photoelectron Spectroscopic Binding Energies

compd	binding energies, eV				
	Cu(2p _{3/2})	I(3d _{5/2})	Co(2p _{3/2})	S(2p)	N(1s)
Cu	932.8				
CuI	932.0	619.4			
Co(S ₂ CN(CH ₂) ₄) ₃			779.4	161.9	399.3
2	932.1	618.6	779.3	162.5	399.7

is both complex and interesting. In space group $I\bar{4}3d$ there are 16 Wyckoff *c* sites of 3 symmetry associated with the cobalt atoms, comprising two sets of opposite chirality, denoted A and B in Figure 2. The network of this figure may be dissected into two totally independent three-dimensional meshes associated with each of the two types of cobalt dithiocarbamate. Within either one of the two polymers all cobalt environments are of the same chirality. The CuI_2Cu dimer in **2** is appreciably bent with a dihedral angle of 35.9° at the I₂ line contrasting with the planar moieties found in $\{[\text{CuI}][\text{Co}(\text{S}_2\text{CN}-n\text{-Pr}_2)_3]\}_2$ (**4**) and $\{[\text{CuI}][\text{Co}(\text{S}_2\text{CN}-i\text{-Pr}_2)_3]\}_2$ (**5**).³ However, there is very little difference overall in the dimer geometries of the three complexes (Table IV).

In this compound, although all six sulfur atoms are coordinated to copper, the two independent Co-S distances of 2.259 (1) and 2.304 (5) Å are markedly different and comparable to the range of 2.258 (2)-2.307 (2) Å found in **3** where only one S...S site is chelated to the copper halide dimer. These results indicate that coordination to the copper halide alone is not the primary condition leading to variations in the Co-S distances found for these compounds and that overall packing requirements of the lattice are likely to be just as important.

X-ray Photoelectron Spectroscopy. In the X-ray photoelectron spectrum of **2**, the binding energies of the Cu(2p) manifold were not significantly different from those observed for CuI with binding energy values of 932.1 and 932.0 eV for the Cu(2p_{3/2}) bands. Similarly, the Co(2p) bands were found to be virtually identical for **2** and $\text{Co}(\text{S}_2\text{CN}(\text{CH}_2)_4)_3$ (Table V). In the S(2p) band, the binding energies increased from 161.9 to 162.5 eV on adduct formation. For comparison, differences in the binding energies between ionic dithiocarbamate salts and the corresponding cobalt complexes are ca. 1.0 eV with a value of 161.0 eV being recorded for $\text{Na}[\text{S}_2\text{CN}(\text{CH}_2)_4]$ and 160.9 eV for $[\text{Co}(\text{diNOsar})][\text{S}_2\text{CN}(\text{CH}_2)_4]_3$.⁹ For $[\text{Co}_2(\text{S}_2\text{CNET}_2)_5][\text{BF}_4]$ in which the dithiocarbamate ligands also bridge between two metal atoms,¹⁰ the S(2p) binding energy was found to be 162.2 eV. These shifts are small but consistently to higher binding energies as the number of atoms coordinated to the sulfur atoms increases. Similarly, the I(3d_{5/2}) peak shifts from 619.4 eV for CuI where the iodide atom is coordinated to four copper atoms to 618.6 eV in **2** where the iodide is coordinated to only two copper atoms.

Increased binding energies usually reflect decreased electron density on the atom concerned, and the effects observed here are

consistent with a transfer of electron density away from the sulfur or iodide atoms as the coordination number increases.

Acknowledgment. We gratefully acknowledge support of this work by a grant from the Australian Research Grant Scheme. The PHI 560 XPS instrument is operated by the Brisbane Surface Analysis Facility, and we are grateful to the BSAF for instrumental time. We thank B. Wood and D. Weedon for helpful discussions. We thank Dr. L. Gahan for kindly preparing the sample of $[\text{Co}_2(\text{S}_2\text{CNET}_2)_5]\text{BF}_4$ used in the XPS measurements. Analyses were carried out by the University of Queensland Microanalytical Service.

Registry No. **1**, 114132-45-5; **2**, 114132-46-6; $\text{Co}(\text{S}_2\text{CNET}_2)_3$, 13963-60-5; $\text{Co}(\text{S}_2\text{CN}(\text{CH}_2)_4)_3$, 24412-38-2; CuI, 7681-65-4.

Supplementary Material Available: Tables SUP-I-SUP-VI, listing thermal and hydrogen parameters and ligand geometries (6 pages); tables of calculated and observed structure factor amplitudes (14 pages). Ordering information is given on any current masthead page.

Contribution from the Department of Chemistry, University of Houston, Houston, Texas 77004

Synthesis, Electrochemistry, and Spectroelectrochemistry of (P)Ge(Fc)₂ and (P)Ge(C₆H₅)(Fc): First Example of Metal-Carbon-σ-Bonded Porphyrins with Two Different Axial Groups

Q. Y. Xu, J.-M. Barbe,¹ and K. M. Kadish*

Received January 20, 1988

In a preliminary communication the oxidative electrochemistry of (OEP)Ge(Fc)₂ in methylene chloride was reported where OEP is the dianion of octaethylporphyrin and Fc is a σ -bonded ferrocenyl group.² The half-wave potential for the first oxidation of this complex is negatively shifted by up to 350 mV with respect to $E_{1/2}$ for oxidation of free ferrocene under the same solution conditions. The electrooxidized $[(\text{OEP})\text{Ge}(\text{Fc})_2]^{2+}$ and $[(\text{OEP})\text{Ge}(\text{Fc})_2]^{2+}$ cations were stable due to a delocalization of positive charge that occurs from the axial ferrocenyl group onto the porphyrin macrocycle. It was not clear if this stability would also be observed for (P)Ge(Fc)₂ complexes with other less basic porphyrin macrocycles or for σ -bonded Fc complexes of the type (P)Ge(R)(Fc) where R is an aryl or alkyl group. This is investigated in the present paper, which describes the detailed electrochemistry and spectroelectrochemistry of (P)Ge(Fc)₂ and (P)Ge(C₆H₅)(Fc), where P is the dianion of octaethylporphyrin (OEP) or tetraphenylporphyrin (TPP). The (P)Ge(C₆H₅)(Fc) complexes represent the first examples of metalloporphyrins

(9) Gahan, L. R.; Healy, P. C.; Weedon, D., unpublished data.

(10) Hendrickson, A. R.; Martin, R. L.; Taylor, D. *J. Chem. Soc., Dalton Trans.* 1975, 2182.

(1) On leave of absence from Laboratoire de Synthèse et d'Electrosynthèse Organométallique, Faculté des Sciences "Gabriel", 6, bd Gabriel, 21100 Dijon, France.

(2) Kadish, K. M.; Xu, Q. Y.; Barbe, J.-M. *Inorg. Chem.* 1987, 26, 2565.

Table I. UV-Visible Data for (P)Ge(Fc)₂, (P)Ge(C₆H₅)Fc, and Related Ge(IV) Porphyrins in PhCN

compd	λ_{\max} , nm ($\epsilon \times 10^{-4}$ cm ⁻¹ M ⁻¹)					
	N(0,0)	B(1,0)	B(0,0)	Q(2,0)	Q(1,0)	Q(0,0)
(OEP)Ge(C ₆ H ₅) ₂ ^a	354 (4.5)	430 (7.2)	442 (35.1)	525 (0.3)	565 (1.7)	600 (0.2)
(OEP)Ge(C ₆ H ₅)Cl ^a	354 (4.2)	413 (4.7)	429 (21.9)	511 (0.2)	552 (1.6)	586 (0.7)
(OEP)Ge(C ₆ H ₅)Fc	357 (4.3)	430 (5.9)	442 (20.4)		569 (1.3)	
(OEP)Ge(Fc) ₂	357 (3.0)	438 (3.5)	440 (14.1)		570 (0.6)	
(TPP)Ge(C ₆ H ₅) ₂ ^a		428 (5.1)	451 (43.3)	559 (0.3)	596 (1.2)	641 (2.8)
(TPP)Ge(C ₆ H ₅)Cl ^a		417 (2.7)	439 (24.5)	532 (0.4)	574 (1.0)	616 (1.1)
(TPP)Ge(C ₆ H ₅)Fc		427 (3.2)	450 (26.4)	556 (0.2)	597 (0.7)	642 (1.3)
(TPP)Ge(Fc) ₂		429 (5.7)	448 (17.3)	559 (0.4)	598 (0.6)	644 (0.7)

^a From ref 5.**Table II.** ¹H NMR Data for (P)Ge(Fc)₂, (P)Ge(C₆H₅)Fc, and (P)Ge(C₆H₅)Cl in CDCl₃ (300 MHz)^a

porphyrin	axial ligands				protons of axial ligands				protons of R ₃		protons of R ₄	
	R ₁		R ₃	R ₄	R ₁		R ₂		m/i	δ	m/i	δ
	R ₁	R ₂			m/i	δ	m/i	δ				
OEP	C ₆ H ₅ ^b	Cl ^b	H	C ₂ H ₅	d/2	0.43			s/4	10.30	t/24	1.95
					t/2	4.86			q/16	4.13		
					t/1	5.39						
	C ₆ H ₅	Fc	H	C ₂ H ₅	d/2	-0.18	m/2	-2.67	s/4	10.16	m/32 ^c	1.93
					t/2	4.56	other signals overlapped				m/16	4.11
					t/1	5.10						
Fc ^d	Fc ^d	H	C ₂ H ₅			m/4	-2.33	s/4	10.14	m/34 ^c	1.96	
						m/4	1.74			q/16	4.15	
						other signals overlapped						
TPP	C ₆ H ₅ ^b	Cl ^b	C ₆ H ₅	H	d/2	0.80			m/12	7.76	s/4	9.03
					t/2	5.05			m/4	8.06		
					t/1	5.54			m/4	8.30		
	C ₆ H ₅	Fc	C ₆ H ₅	H	d/2	0.38	m/2	-2.23	m/12	7.74	s/4	8.91
					t/2	4.83	m/2	1.74	m/8	8.19		
					t/1	5.32	s/5	1.99				
	Fc	Fc	C ₆ H ₅	H			m/4	-2.22	m/12	7.66	s/4	8.79
							m/4	1.74	m/8	8.14		
							s/10	1.98				

^a Key: R₁ = axial ligand; R₂ = axial ligand; R₃ = porphyrin methinic group; R₄ = porphyrin pyrrole group; m = multiplicity; i = number of protons; s = singlet; d = doublet; t = triplet; q = quartet; m = multiplet. ^b Reference 5. ^c Signal due to the resonance of -CH₃ porphyrinic protons and ferrocenyl protons. ^d Reference 2.

containing two different metal-carbon- σ -bonded axial groups.

Experimental Section

Chemicals. All solvents were thoroughly dried and distilled under nitrogen prior to use. Spectroanalyzed grade methylene chloride (CH₂Cl₂, Aldrich) was distilled from CaH₂ under nitrogen. Reagent grade benzonitrile (PhCN, Aldrich) was distilled from P₂O₅ under reduced pressure. Tetra-*n*-butylammonium perchlorate (TBAP) from Alfa was recrystallized twice from ethanol.

Preparation of (P)Ge(C₆H₅)(Fc) and (P)Ge(Fc)₂. (P)Ge(Fc)₂ and (P)Ge(C₆H₅)(Fc) were synthesized under nitrogen by Schlenk techniques. The starting materials, (P)GeCl₂ and (P)Ge(C₆H₅)Cl, were obtained by synthetic methods described in the literature.³⁻⁶ In a typical experiment 0.1 mmol of (P)Ge(C₆H₅)Cl⁵ in 40 mL of benzene and 0.72 mmol of FcLi (obtained from the reaction of 0.72 mmol of *n*-BuLi in hexane with 0.72 mmol of bromoferrocene in 5 mL of anhydrous diethyl ether) were allowed to react for 30 min at room temperature. After hydrolysis with 10 mL of degassed water, the solution was evaporated under vacuum. Purification of the resulting solid was achieved by column chromatography (neutral alumina, activity 1) using toluene in the dark. The yield was about 40%.

Instrumentation. ¹H NMR spectra were recorded on a Nicolet NT-300 spectrometer controlled by a Model 293.C programmer. IR spectra were recorded with an IBM FTIR 32 spectrometer coupled with an IBM Model 9000 microcomputer. Samples were prepared as 1% dispersions in CsI.

Electronic absorption spectra were recorded in PhCN or CH₂Cl₂ on either an IBM Model 9430 spectrophotometer or a Tracor Northern 1710 holographic optical spectrometer multichannel analyzer (1.2 nm

resolution). ESR spectra were recorded at 115 K on an IBM Model ER 100D spectrometer equipped with a microwave ER-040-X bridge and an ER 080 power supply. The *g* values were measured with respect to diphenylpicrylhydrazyl (*g* = 2.0036 ± 0.0003).

Cyclic voltammetric measurements were obtained with a three-electrode system utilizing a Pt-button working electrode (0.2 mm²), a Pt-wire counter electrode, and an SCE reference electrode. An IBM EC 225 voltammetric analyzer and an EG&G Princeton Applied Research Model 174A/175 polarographic analyzer/potentiostat were used to measure the current-voltage curves. Controlled-potential electrolysis was performed by using an EG&G Model 173 potentiostat. The reference and the counter electrodes were separated from the bulk solution by a fritted-glass bridge. An IBM EC 225 voltammetric analyzer coupled with a Tracor Northern 1710 holographic optical spectrometer multichannel analyzer gave time-resolved spectral data with use of an optically transparent thin-layer electrode (OTTLE).⁷

Results and Discussion

Spectroscopic Properties of (P)Ge(Fc)₂ and (P)Ge(C₆H₅)(Fc). Each complex was characterized by UV-visible, IR, and ¹H NMR spectroscopy. Figure 1 shows the electronic absorption spectra of (TPP)Ge(C₆H₅)₂, (TPP)Ge(C₆H₅)(Fc), and (TPP)Ge(Fc)₂ in PhCN. A large decrease in molar absorptivities is observed, and there is a slight blue shift of the Soret band absorbance maximum upon going from the σ -bonded diphenyl complex to the σ -bonded monophenyl monoferrocenyl complex and finally to the σ -bonded diferrocenyl complex. This is also illustrated in Table I which summarizes the UV-visible data of the OEP and TPP derivatives.

¹H NMR data for (P)Ge(C₆H₅)Cl, (P)Ge(C₆H₅)(Fc), and (P)Ge(Fc)₂ in CDCl₃ are given in Table II. The ¹H NMR spectrum of (TPP)Ge(Fc)₂ is in good agreement with published values of this complex.⁴ The (OEP)Ge(Fc)₂ complex shows a

(3) Guillard, R.; Lecomte, C.; Kadish, K. M. *Struct. Bonding (Berlin)* **1987**, *64*, 205-268.

(4) Maskasky, J. E.; Kenney, M. E. *J. Am. Chem. Soc.* **1971**, *93*, 2060.

(5) Kadish, K. M.; Xu, Q. Y.; Barbe, J.-M.; Anderson, J. E.; Wang, E.; Guillard, R. *J. Am. Chem. Soc.* **1987**, *109*, 7705.

(6) Maskasky, J. E.; Kenney, M. E. *J. Am. Chem. Soc.* **1973**, *95*, 1443.

(7) Lin, X. Q.; Kadish, K. M. *Anal. Chem.* **1985**, *57*, 1498.

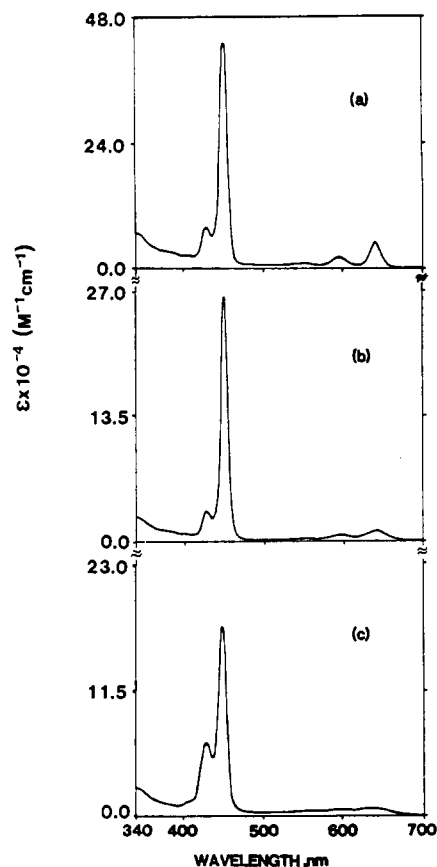


Figure 1. Electronic absorption spectra of (a) 3.7×10^{-4} M (TPP)Ge(C_6H_5)₂, (b) 7.4×10^{-4} M (TPP)Ge(C_6H_5)(Fc), and (c) 8.7×10^{-4} M (TPP)Ge(Fc)₂ in PhCN.

Table III. IR Data (cm^{-1}) for (P)Ge(Fc)₂, (P)Ge(C_6H_5)Fc, and Related Ge(IV) Porphyrins in CsI Pellets

compd	Ge-Cl	Ge-C
(OEP)GeCl ₂	314	
(OEP)Ge(C_6H_5) ₂ ^a		365
(OEP)Ge(C_6H_5)Cl ^a	305	355
(OEP)Ge(Fc) ₂ ^b		350
(OEP)Ge(C_6H_5)Fc		361 ^c
(TPP)GeCl ₂	341	
(TPP)Ge(C_6H_5) ₂ ^a		340
(TPP)Ge(C_6H_5)Cl ^a	<i>d</i>	<i>d</i>
(TPP)Ge(Fc) ₂		330
(TPP)Ge(C_6H_5)Fc		338 ^c

^a Reference 5. ^b Reference 2. ^c Only one ν_{Ge-C} observed. ^d A single vibration was detected at 314 cm^{-1} and could correspond to either ν_{Ge-Cl} or ν_{Ge-C} .

quartet for the methylenic protons, while the asymmetrical coordination of (OEP)Ge(C_6H_5)(Fc) leads to the presence of a multiplet for the same signal. The ¹H NMR spectrum of (TPP)Ge(C_6H_5)(Fc) is illustrated in Figure 2. Integration of the proton signals gives a ratio of one ferrocenyl group to one phenyl group on the complex. The chemical shifts of the ferrocenyl

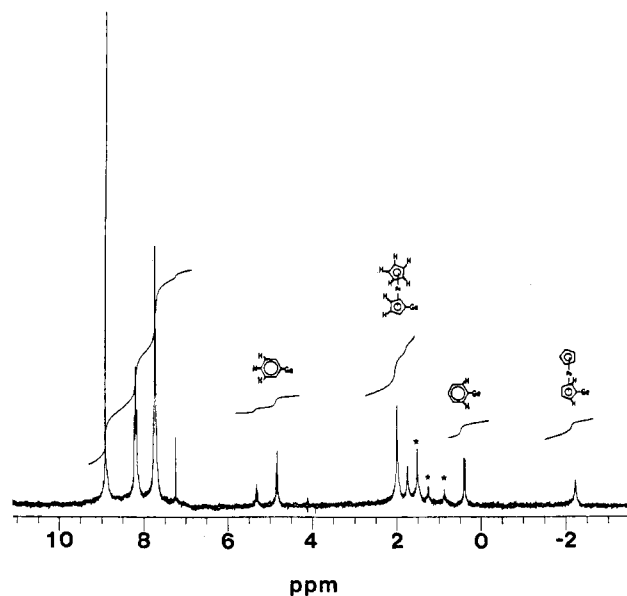


Figure 2. ¹H NMR spectrum of (TPP)Ge(C_6H_5)(Fc) at 300 MHz in $CDCl_3$ (* indicates impurities). Only the peaks from protons of the axial ligands are labeled.

protons on (TPP)Ge(C_6H_5)(Fc) are identical with those on (TPP)Ge(Fc)₂, while the phenyl protons are only slightly shielded with respect to those of (TPP)Ge(C_6H_5)₂.⁵

An electron-withdrawing effect of the axial Fc ligand on the pyrrolic or methinic protons is observed from the ¹H NMR spectral data. The chemical shift of the methinic proton is 10.30 ppm for (OEP)Ge(C_6H_5)Cl, 10.16 ppm for (OEP)Ge(C_6H_5)(Fc), and 10.14 ppm for (OEP)Ge(Fc)₂, and this order agrees with an increase in the electron-withdrawing ability of the corresponding axial ligands. The same trend in chemical shifts of the pyrrole proton is obtained for complexes in the TPP series (see Table II).

Table III summarizes the IR data below 400 cm^{-1} for (P)Ge(Fc)₂ and (P)Ge(C_6H_5)Fc as well as for the starting Ge(IV) materials. The germanium-carbon stretch occurs at 350 cm^{-1} for (OEP)Ge(Fc)₂ and at 330 cm^{-1} for (TPP)Ge(Fc)₂. These values agree with reported metal-carbon stretches of (P)Ge(C_6H_5)₂.⁵ Only one Ge-C vibrational frequency is found for (P)Ge(C_6H_5)(Fc).

Oxidation of (OEP)Ge(Fc)₂ and (TPP)Ge(Fc)₂. The oxidative electrochemistry of (OEP)Ge(Fc)₂ has been reported in CH_2Cl_2 ,² and similar results are obtained in PhCN. (OEP)Ge(Fc)₂ undergoes two reversible electrooxidations in the potential range of PhCN (see Figure 3a). These are at $E_{1/2} = +0.17$ and $+0.34$ V and occur at the two σ -bonded ferrocenyl groups. An anodic peak at $E_{pa} = +1.30$ V overlaps with a discharge of the PhCN solvent, but the reaction is well-defined in CH_2Cl_2 and is believed to involve an oxidation of the porphyrin π ring system. An additional small reversible oxidation at $+0.62$ V in PhCN is attributed to oxidation of bromoferrocene, which remains as a residual impurity from the synthesis. This was verified by adding genuine samples of bromoferrocene to the solution.

Similar oxidative behavior is observed for (TPP)Ge(Fc)₂ in PhCN (see Figure 3c). However, there is the expected 90–100-mV

Table IV. Half-Wave Potentials (V vs. SCE) of (P)Ge(Fc)₂ and (P)Ge(C_6H_5)Fc in CH_2Cl_2 and PhCN, 0.1 M TBAP

complex	solvent	oxidn		redn
		Fc ligand(s)	porphyrin ring	porphyrin ring
(OEP)Ge(Fc) ₂	CH_2Cl_2 ^a	0.14, 0.32	1.32, 1.57 ^b	-1.59
	PhCN	0.17, 0.34	1.30 ^b	-1.49
(OEP)Ge(C_6H_5)Fc	PhCN	0.22	1.13 ^b	-1.44
(OEP)Ge(C_6H_5) ₂ ^c	PhCN		0.88, ^b 1.39	-1.40
(TPP)Ge(Fc) ₂	PhCN	0.27, 0.43	1.40 ^b	-1.15, -1.71
(TPP)Ge(C_6H_5)Fc	PhCN	0.29	1.24, ^b 1.51	-1.15, -1.70
(TPP)Ge(C_6H_5) ₂ ^c	PhCN		0.95, ^b 1.45 ^b	-1.10, -1.65

^a From ref 2. ^b E_{pa} measured at 0.1 V/s. ^c From ref 5.

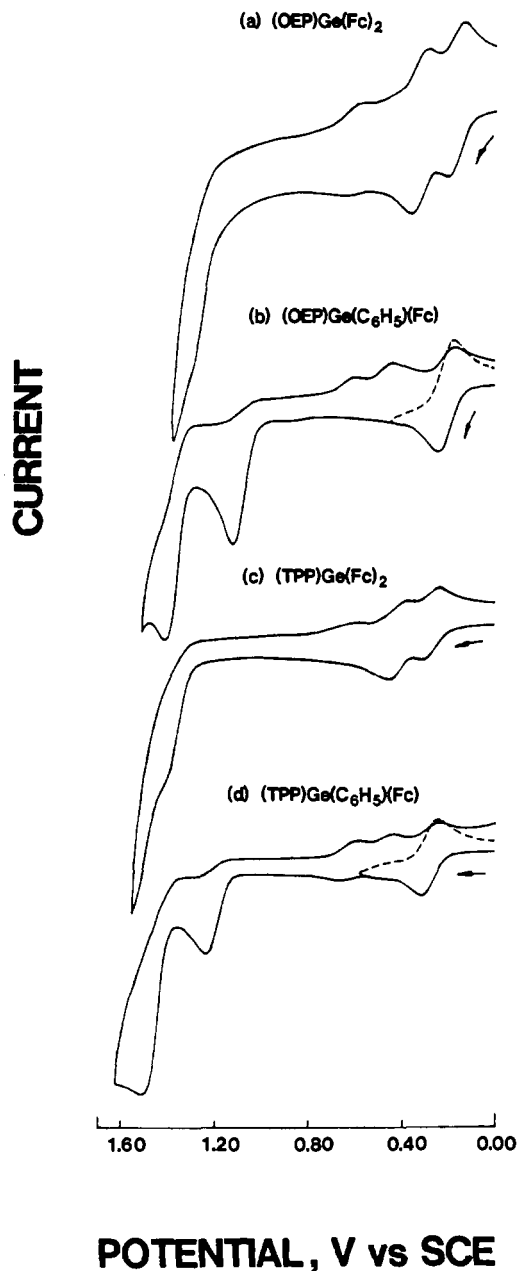


Figure 3. Cyclic voltammograms of $\sim 10^{-3}$ M (a) (OEP)Ge(Fc)₂, (b) (OEP)Ge(C₆H₅)(Fc), (c) (TPP)Ge(Fc)₂, and (d) (TPP)Ge(C₆H₅)(Fc) in PhCN, 0.1 M TBAP.

negative shift of the Fc oxidation half-wave potentials. This is due to the increased basicity of OEP with respect to that of TPP.

Half-wave potentials for oxidation of each (P)Ge(Fc)₂ complex are listed in Table IV. Potential differences between the first and second oxidations of (P)Ge(Fc)₂ range between 0.16 and 0.18 V and agree with separations of 0.17–0.20 V for Fc–Si(CH₃)₂–Fc,⁸ Fc–Se–Fc,⁹ and Fc–CH₂–Fc⁹ in CH₂Cl₂ or CH₃CN. Therefore, on the basis of this similarity between (P)Ge(Fc)₂ and other ferrocene derivatives, an interaction between the two iron centers of (P)Ge(Fc)₂ can be deduced.^{2,10}

Time-resolved thin-layer spectra were recorded during the first three one-electron oxidations of each (P)Ge(Fc)₂ complex, and wavelengths of maximum absorbance for each electrogenerated complex are summarized in Table V. The blue shift and large

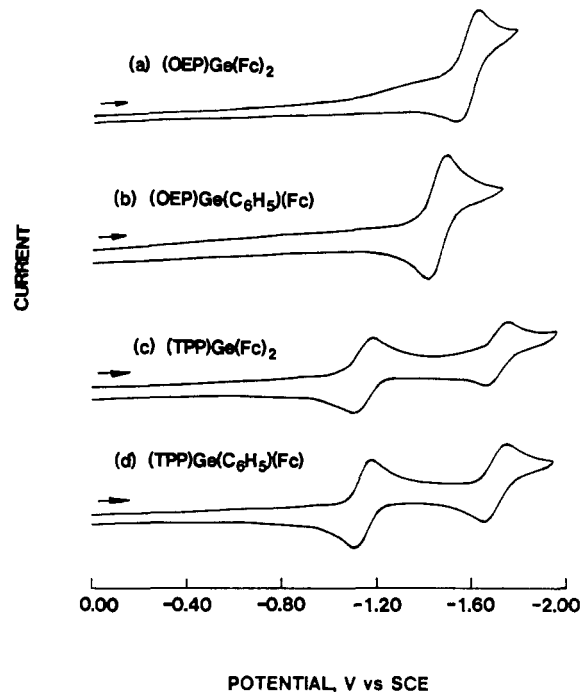
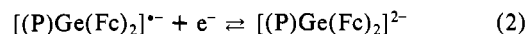
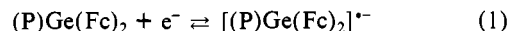


Figure 4. Cyclic voltammograms of $\sim 10^{-3}$ M (a) (OEP)Ge(Fc)₂, (b) (OEP)Ge(C₆H₅)(Fc), (c) (TPP)Ge(Fc)₂, and (d) (TPP)Ge(C₆H₅)(Fc) in PhCN, 0.1 M TBAP.

decrease in the Soret band intensity during both the first and second oxidations of these complexes can be ascribed to a partial delocalization of positive charge on the a_{1u} and a_{2u} orbitals of the porphyrin macrocycle.²

The abstraction of a third electron from (P)Ge(Fc)₂ results in a loss of one Fc unit on the spectroelectrochemical time scale (2–5 min). This results in a dramatic change in both the Soret band and Q-band regions. Similar spectral changes accompanying the Ge–C bond cleavage occur during oxidation of (P)Ge(R)₂ where R is an alkyl or aryl group.⁵ Therefore, on the basis of these similarities, the final species generated from solutions of (P)Ge(Fc)₂ is assigned as [(P)Ge(Fc)ClO₄]⁺.

Reduction of (OEP)Ge(Fc)₂ and (TPP)Ge(Fc)₂ in PhCN. (P)Ge(Fc)₂ is reversibly reduced in either one or two steps depending upon the type of porphyrin macrocycle. (OEP)Ge(Fc)₂ (Figure 4a) undergoes one reversible reduction, while (TPP)Ge(Fc)₂ (Figure 4c) undergoes two reversible reductions in PhCN.



Thin-layer spectral changes upon the first electroreduction of (OEP)Ge(Fc)₂ are shown in Table V. The Soret band at 439 nm decreases, and a new peak appears at 466 nm. At the same time, the single peak at 569 nm disappears and peaks at 733 and 849 nm, which are indicative of a porphyrin ring π anion radical,^{11,12} appear (see Figure 5a). The singly reduced (TPP)Ge(Fc)₂ complexes undergo similar spectral changes, and a summary of these data is listed in Table V.

Oxidation of (OEP)Ge(C₆H₅)(Fc) and (TPP)Ge(C₆H₅)(Fc) in PhCN. Cyclic voltammograms for oxidation of the (P)Ge(C₆H₅)(Fc) complexes in PhCN are presented in Figure 3. Half-wave potentials for oxidation of each complex are listed in Table IV. Low Soret band molar absorptivities for the (P)Ge(C₆H₅)(Fc) complexes are observed and indicate a delocalization of charge from the single Fc ligand to the porphyrin π ring system. Half-wave potentials for the first reversible oxidation confirm this. The oxidations of (OEP)Ge(C₆H₅)(Fc) (Figure 3b) at 0.22 V and

(8) Bocarsly, A. B.; Walton, E. G.; Bradley, M. G.; Wrighton, M. S. *J. Electroanal. Chem. Interfacial Electrochem.* **1979**, *100*, 283.

(9) Shu, P.; Bechgaard, K.; Cowan, D. O. *J. Organomet. Chem.* **1976**, *41*, 1849.

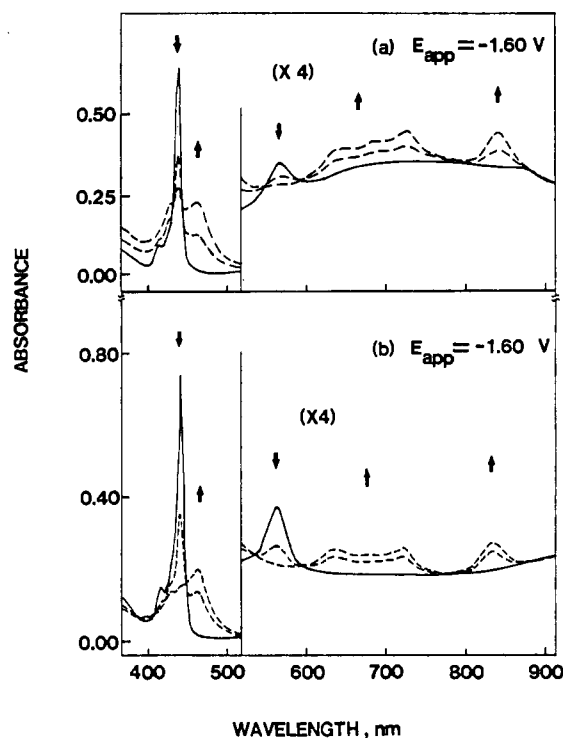
(10) Yap, W. T.; Durst, R. A. *J. Electroanal. Chem. Interfacial Electrochem.* **1981**, *130*, 3.

(11) Felton, R. H. In *The Porphyrins*; Dolphin, D., Ed.; Academic: New York, 1978; Vol. V, Chapter 3.

(12) Kadish, K. M. *Prog. Inorg. Chem.* **1986**, *34*, 435–605.

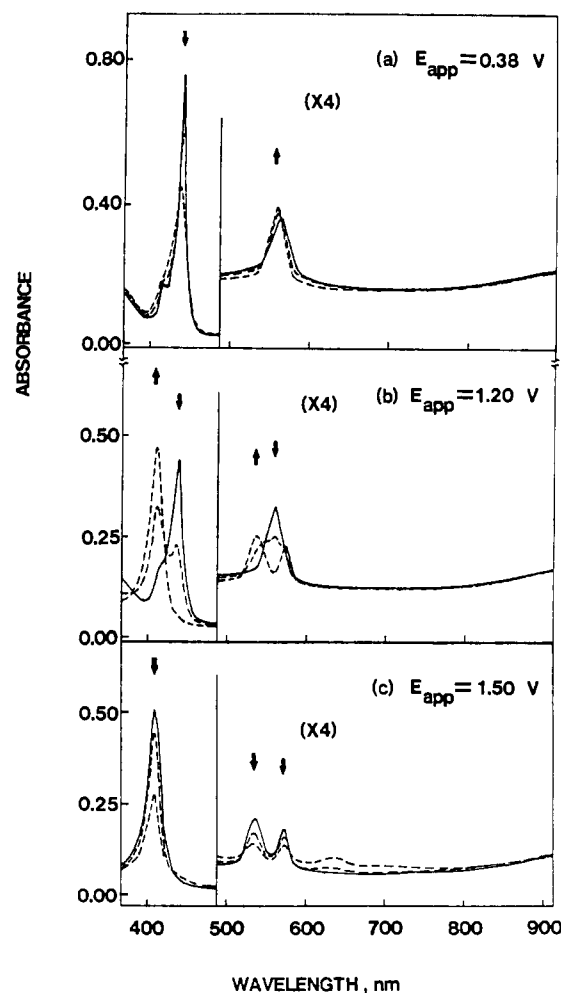
Table V. Maximum Absorbance Wavelengths and Corresponding Molar Absorptivities of (P)Ge(Fc)₂ and (P)Ge(C₆H₅)Fc in CH₂Cl₂ or PhCN, Containing 0.2 M TBAP

complex	solvent	reacn	λ_{\max} , nm ($\epsilon \times 10^{-4}$ cm ⁻¹ M ⁻¹)		
(OEP)Ge(Fc) ₂	CH ₂ Cl ₂ ^a	none	439 (14.1)	569 (0.6)	
		1e oxidn	435 (8.0)	561 (0.6)	
		2e oxidn	434 (5.9)	559 (0.9)	
		3e oxidn	408 (6.1)	537 (0.1)	578 (0.04)
		1e redn	466 (5.2)	733 (0.8)	849 (0.8)
(OEP)Ge(C ₆ H ₅)Fc	PhCN	none	443 (20.4)	569 (1.3)	
		1e oxidn	439 (11.8)	565 (1.5)	
		2e oxidn	412 (14.0)	542 (1.0)	580 (0.9)
		3e oxidn	411 (7.6)	644 (0.5)	
		1e redn	465 (5.6)	641 (0.5)	732 (0.5) 846 (0.6)
(TPP)Ge(Fc) ₂	PhCN	none	449 (17.3)	597 (0.6)	641 (0.7)
		1e oxidn	448 (11.2)	591 (0.6)	633 (0.9)
		2e oxidn	448 (10.2)	588 (0.7)	633 (1.2)
		3e oxidn	433 (8.9)	554 (0.6)	633 (0.7)
		1e redn	484 (4.9)	642 (0.8)	832 (0.7)
(TPP)Ge(C ₆ H ₅)Fc	PhCN	none	450 (26.4)	596 (0.7)	642 (1.3)
		1e oxidn	450 (18.3)	592 (0.8)	636 (1.8)
		2e oxidn	431 (15.9)	556 (0.7)	634 (0.6)
		1e redn	485 (6.3)		825 (1.2)

^a From reference 2.**Figure 5.** Time-resolved spectra during controlled-potential reduction of (a) (OEP)Ge(Fc)₂ at -1.60 V and (b) (OEP)Ge(C₆H₅)Fc at -1.60 V in PhCN, 0.2 M TBAP.

(TPP)Ge(C₆H₅)(Fc) (Figure 3d) at 0.29 V can be compared to $E_{1/2}$ values of 0.17 and 0.27 for oxidation of (OEP)Ge(Fc)₂ and (TPP)Ge(Fc)₂ in PhCN (Figure 3a,c). In contrast, free ferrocene is oxidized at $E_{1/2} = 0.47$ V in PhCN. (The two small peaks at E_{pc} of 0.44 and 0.62 V in Figure 3b correspond to the oxidation of trace ferrocene and bromoferrocene.) The electrochemistry of (TPP)Ge(C₆H₅)(Fc) is similar to that of (OEP)Ge(C₆H₅)(Fc).

Figure 6 illustrates time-resolved electronic absorption spectra obtained during oxidation of (OEP)Ge(C₆H₅)(Fc) in PhCN. The final species after oxidation at 0.38 V has a Soret band that is decreased in peak intensity by approximately 50% and blue-shifted from 443 to 439 nm (see Figure 6a). The Q-band intensity increases slightly and shifts from 569 to 565 nm during this reaction. Four well-defined isosbestic points are present at 437, 450, 545, and 567 nm, suggesting that only two species, (OEP)Ge(C₆H₅)(Fc) and [(OEP)Ge(C₆H₅)(Fc)]⁺, are in equilibrium.

**Figure 6.** Time-resolved spectra during controlled-potential oxidation of (OEP)Ge(C₆H₅)(Fc) in PhCN, 0.2 M TBAP at (a) 0.38 V, (b) 1.20 V, and (c) 1.50 V.

More dramatic spectral changes are observed during controlled-potential oxidation of [(OEP)Ge(C₆H₅)(Fc)]⁺ at 1.20 V. The final solution spectrum is characterized by a Soret band at 412 nm and two Q-bands at 542 and 580 nm and is similar to the spectrum that results after removal of three electrons from (OEP)Ge(Fc)₂ in CH₂Cl₂ containing 0.1 M TBAP (see Table V). No isosbestic points are observed during this process, indicating that more than two species are present in solution (see Figure 6b).

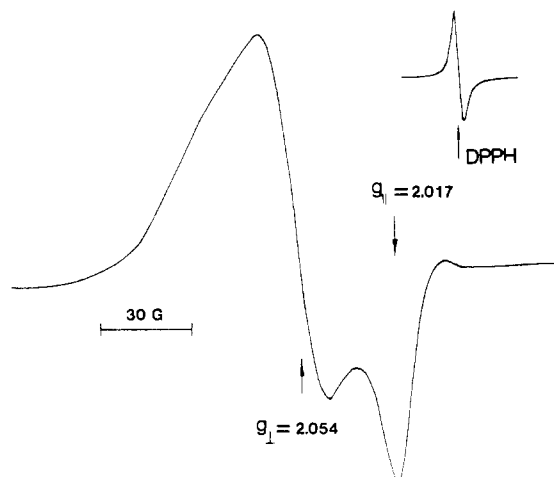


Figure 7. ESR spectrum of doubly oxidized (OEP)Ge(Fc)₂ at 115 K in PhCN, 0.2 M TBAP.

Thus, the final species in solution may be assigned as [(OEP)Ge(Fc)ClO₄]⁺ resulting from the cleavage of one germanium-phenyl bond. Finally, a porphyrin π cation radical is formed after abstraction of one electron from the proposed [(OEP)Ge(Fc)ClO₄]⁺ complex (see Figure 6c). Oxidized (TPP)Ge(C₆H₅)(Fc) shows similar spectroelectrochemical changes, and these spectral data are summarized in Table V.

Reduction of (OEP)Ge(C₆H₅)(Fc) and (TPP)Ge(C₆H₅)(Fc). (OEP)Ge(C₆H₅)(Fc) is reduced at a potential 50 mV positive of (OEP)Ge(Fc)₂ (see Figure 4), but the half-wave potentials for reduction of (TPP)Ge(C₆H₅)(Fc) and (TPP)Ge(Fc)₂ are identical within experimental error (Table IV). Time-resolved thin-layer spectra obtained during reduction of (OEP)Ge(C₆H₅)(Fc) follow the trends for formation of a π anion radical.^{11,12} These spectral changes are shown in Figure 5b. The Soret band at 443 nm and a Q-band at 569 nm disappear after addition of one electron to the complex while new peaks appear at 465, 641, 732, and 846 nm. Four well-defined isosbestic points are present, indicating that only two species, (OEP)Ge(C₆H₅)(Fc) and [(OEP)Ge(C₆H₅)(Fc)]⁻, are in equilibrium. Similar electronic absorption spectral changes are obtained upon reduction of (TPP)Ge(C₆H₅)(Fc), and these data are summarized in Table V.

ESR Spectra of Oxidized (OEP)Ge(Fc)₂ in PhCN, 0.2 M TBAP. No ESR signal is detected after exhaustive bulk electrolysis of (OEP)Ge(Fc)₂ at +0.21 V. This is presumably due to the interaction between the oxidized ferrocenyl group and the porphyrin π ring system. However, an anisotropic ESR spectrum is obtained after controlled-potential electrolysis at 0.42 V (the second oxidation). This signal is shown in Figure 7 and is characterized by $g_{\perp} = 2.054$ and $g_{\parallel} = 2.017$. It is worth noting that this spectrum shows some features similar to those of singly oxidized biferrocenylene,¹³ [Fe₂(C₅H₄)₄]⁺, where the unpaired electron is rapidly exchanging between the two iron centers.¹⁴

Comparisons may be made between the ESR spectrum of [(OEP)Ge(Fc)₂]²⁺ and that of the ferrocenium cation or singly oxidized biferrocenylene.¹³ No downfield absorption band ($g = 3.20$ – 4.35) is observed for the ferrocenium cation in [(OEP)Ge(Fc)₂]²⁺. This might suggest that the charge on a ferrocenyl ligand is less than unity. The similarity in shape of the ESR spectrum for [(OEP)Ge(Fc)₂]²⁺ to that of the upfield absorption band of the singly oxidized biferrocenylene might be additional evidence for a rapid exchange of the electron between the two iron atoms of the oxidized metalloporphyrin.

Comparison of (P)Ge(Fc)₂ and (P)Ge(C₆H₅)(Fc) with Other (P)Ge(R)₂ Complexes. The (P)Ge(C₆H₅)(Fc) complexes provide the first synthetic examples of metalloporphyrins containing two different metal-carbon- σ -bonded axial groups. The physico-

chemical properties of neutral (P)Ge(Fc)₂ and (P)Ge(C₆H₅)(Fc) are similar to other σ -bonded (P)Ge(R)₂ complexes. However, the Fc complexes show an additional unique feature. The Soret band molar absorptivities of (P)Ge(Fc)₂ and (P)Ge(C₆H₅)(Fc) are only about half those of other (P)Ge(R)₂ complexes (see Table I), and this can be unambiguously attributed to a delocalization of electron density from the porphyrin macrocycle onto the ferrocenyl group. As a consequence, the germanium-carbon σ -bonds in (P)Ge(Fc)₂ and (P)Ge(C₆H₅)(Fc) are much more stable than the metal-carbon bonds in other (P)Ge(R)₂ complexes.

The enhanced stability of [(P)Ge(C₆H₅)(Fc)]⁺ with respect to the highly reactive [(P)Ge(C₆H₅)₂]⁺ complex⁵ results from delocalization of positive charge onto the porphyrin macrocycle. This delocalization effect (with respect to Fc⁺/Fc) amounts to -180 mV for [(TPP)Ge(C₆H₅)(Fc)]⁺ and -250 mV for [(OEP)Ge(C₆H₅)(Fc)]⁺. For [(P)Ge(Fc)₂]⁺ both a delocalization of positive charge onto the porphyrin macrocycle and an interaction between two iron centers results in greater stabilization. The overall effect with respect to Fc⁺/Fc in PhCN is -250 mV for [(TPP)Ge(Fc)₂]⁺ and -330 mV for [(OEP)Ge(Fc)₂]⁺.

On the other hand, the stability of the metal-carbon σ -bond in the dialkyl- or diarylgermanium(IV) porphyrins of the form (P)Ge(R)₂ can be varied with changes in the degree of electron donation by the axial ligand.⁵ The more electron-withdrawing the R group, the more stable the σ -bond will be and the more positive the first oxidation potential will be. An anodic shift of about 240 mV was observed between the first oxidation peak potential of the (P)Ge(R)₂ complex containing the strongest σ -bonding R group (R = C₆H₅) and that containing the weakest σ -bonding ligand (R = CH₂C₆H₅).⁵

Finally, differences between the stability of [(P)Ge(Fc)₂]⁺ or [(P)Ge(C₆H₅)(Fc)]⁺ and other [(P)Ge(R)₂]⁺ complexes are also related to a difference in the site of oxidation between the two types of complexes. For the former two series of complexes the site of the initial electrooxidation is clearly at the axial ligand position, but this is unclear for the other σ -bonded (P)Ge(R)₂ complexes.

Acknowledgment. The support of the National Science Foundation (Grant No. 8515411) is gratefully acknowledged.

Registry No. (OEP)Ge(Fc)₂, 109335-07-1; (OEP)Ge(C₆H₅)Fc, 114467-16-2; (TPP)Ge(C₆H₅)₂, 110718-65-5; (TPP)Ge(C₆H₅)Fc, 114467-17-3; (TPP)Ge(Fc)₂, 11060-95-0; (OEP)GeCl₂, 31713-45-8; (OEP)Ge(C₆H₅)Cl, 110718-66-6; (TPP)GeCl₂, 41043-38-3; (TPP)Ge(C₆H₅)Cl, 111237-13-9; (OEP)Ge(C₆H₅)₂, 110718-63-3; [(TPP)Ge(Fc)₂]⁻, 114594-51-3; [(TPP)Ge(Fc)₂]²⁻, 114594-52-4; [(OEP)Ge(C₆H₅)(Fc)]⁺, 114674-33-8; [(TPP)Ge(Fc)₂]⁺, 114594-53-5; [(TPP)Ge(C₆H₅)(Fc)]⁺, 114614-03-8; [(OEP)Ge(C₆H₅)(Fc)]⁻, 114594-54-6.

Contribution from the Department of Chemistry and Biochemistry, University of Colorado, Boulder, Colorado 80309

Synthesis and Borane Coordination of Primary Alkenyl- and Alkynylphosphines

Robert H. Shay, Bruce N. Diel, David M. Schubert, and Arlan D. Norman*

Received March 14, 1988

Primary alkenyl- and alkynylphosphines are interesting because they contain, in addition to P(III), \geq P donor, and P-H functionalities, carbon-carbon double and triple bonds. Although these compounds offer considerable potential for organophosphine ligand and extended molecule (oligomer/polymer) synthesis, only HC \equiv CPh₂,¹ MeC(PH₂)=CH₂,² PhCH=CHPh₂,³ and CH₂=

(13) Morrison, W. H., Jr.; Krogsrud, S.; Hendrickson, D. N. *Inorg. Chem.* 1973, 12, 1998.

(14) Prins, R. *Mol. Phys.* 1970, 19, 603.

* To whom correspondence should be addressed.